Optimization-Based Nonimpact Rolling Locomotion of a Variable Geometry Truss

Sumin Park, Eugene Park, Mark Yim, Jongwon Kim, and TaeWon Seo

***Abstract*—A variable geometry truss (VGT) is a modular truss-structured robot consisting of linear actuators and three-degree-of-freedom joints. Having a sophisticated structure, the VGT can easily be damaged when it rolls and impacts the ground. This letter proposes a nonimpact rolling locomotion scheme to avoid VGT damage. It is assumed that the VGT moves quasi-statically and maintains a static stability. There exists a control phase and a rolling phase during locomotion. During the control phase, the VGT can freely move its center of mass within the supporting polygon. During the rolling phase, the VGT's center of mass is fixed at the edge of the support polygon, and it tilts forward until a node touches the ground to make a new support polygon. This algorithm optimizes the velocity of the VGT's nodes at every time step so that the center of mass follows a desired trajectory of rolling motion. A simulation verifies that the algorithm ensures that the VGT maintains its static stability, does not tumble, and accurately follows its desired trajectory.**

***Index Terms*—Variable geometry truss, rolling locomotion, damage prevention.**

I. Introduction

A variable geometry truss (VGT) is a type of modular robot with a truss structure, consisting of linear actuators that act as 3-degrees-of-freedom joint nodes. The VGT schematic is presented in Fig. 1. The structure allows the VGT to flexibly change its geometric shape so that it can be folded into a compact transferrable form and then deployed to achieve its function [1]–[3]. It can also access and adjust to irregular environments, such as narrow spaces or obstacles [4], [5]. Furthermore, using its truss structure, the VGT can efficiently support large loads and perform shoring work [6], [7].

VGT locomotion is achieved by controlling the center of mass by changing the geometric configuration of the VGT, such as during rolling locomotion. This is accomplished by tipping the VGT and contacting the ground in front. There have been several studies performed on rolling motion. Most focused on heuristically developing a gait cycle. Lee *et al.* simulated the rolling locomotion of icosahedral VGTs, giving arc trajectories to each control node, so that it could dynamically roll across the ground [8]. Abrahantes *et al.* simulated tumbling and rolling locomotion of a cube-shaped VGT, giving length profiles to nodes they wanted to move [9], [10]. These methods executed pre-planned motions of nodes so that the VGT could move one gait rotation cycle. Whereas their planning method is intuitive, it can only be applied to pre-planned configurations; it only moves in certain patterns. It cannot move in irregular environments and cannot freely follow arbitrary trajectories.

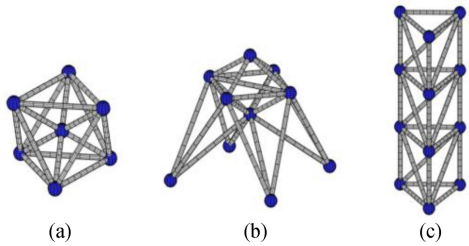

Fig. 1. Schematic of VGT: (a) polyhedron shape for rolling, (b) quadruped shape for walking, and (c) tower shape for shoring.

Another method of locomotion planning is based on optimization algorithms. Usevitch *et al.* proposed a locomotion algorithm, which optimized the velocity of nodes at every time step when the desired VGT trajectory was given [11]. The algorithm was verified by simulating the locomotion of a tetrahedral VGT. Once the optimization algorithm was set up, it could be applied to any VGT configuration. It could also be applied to various trajectories and terrains, because it did not depend on a specific gait cycle.

Although these optimization-based algorithms suggested useful methods for generalizing locomotion, they did not deal with practical rolling-motion problems. When implementing an algorithm in a real case, it is essential to properly design the rolling motion to prevent the VGT from receiving impacts from the ground. When a polyhedron-shaped object, such as dice, rolls across the ground, it repetitively receives impacts. In the case of VGT rolling, this repetitive impacting can cause significant damage to mechanical components, linear actuators, and joints.

In this letter, non-impact rolling algorithms are proposed to eliminate dynamic falling portions of rolling locomotion. The controlled motion of VGT will be slow enough so motions can be

Manuscript received September 9, 2018; accepted December 26, 2018. Date of publication January 11, 2019; date of current version February 4, 2019. This letter was recommended for publication by Associate Editor K. Lee and Editor N. Y. Chong upon evaluation of the reviewers' comments. This work was supported by the Industrial Core Technology Development Project through Ministry of Trade, Industry and Energy, South Korea (MOTIE) under Grant 1006-9072. *(Corresponding author: TaeWon Seo.)*

S. Park, E. Park, and J. Kim are with the School of Mechanical and Aerospace Engineering, Seoul National University, Seoul 08826, South Korea (e-mail: smpark@rodel.snu.ac.kr; eupark@rodel.snu.ac.kr; jongkim@snu.ac.kr).

M. Yim is with the School of Mechanical Engineering and Applied Mechanics, University of Pennsylvania, Philadelphia, PA 19146 USA (e-mail: yim@seas.upenn.edu).

T. W. Seo is with the School of Mechanical Engineering, Hanyang University, Seoul 04763, South Korea (e-mail: taewonseo@hanyang.ac.kr).

Digital Object Identifier 10.1109/LRA.2019.2892596

considered to be quasi-static maintaining static stability. Thus, the VGT is stable when the center of mass projected on the ground is inside the support polygon. Given a desired trajectory, the algorithm optimizes the motion of nodes at every time step. During rolling locomotion, two phases (a control phase and a rolling phase) are defined based on the location of center of mass. By alternating the control and rolling phase, VGT can follow desired trajectory while maintaining stability and preventing ground impact. The detailed algorithm is provided in the following sections and was verified in simulation.

II. Kinematics

A. Configuration and Terminologies

VGT configuration can be defined by the connectivity between nodes and members and its nodes' positions. Connectivity can be mathematically modeled as a graph: $G = (N, E)$. $\mathrm{N} = \{1, 2, \ldots, .n\}$ is a set of nodes, and $E = \{e_1, e_1, \ldots, e_m\}$ is a set of edges or members, where an edge, $e_k = \{i, j\}$, represented as two nodes with connecting edges. The position of node i is represented as $p_i = [p_{ix}, p_{iy}, p_{iz}]^T$. The position of all nodes are represented as $x = [p_{1x}, \ldots, p_{nx}, p_{1y}, \ldots, p_{ny}, p_{1z}, \ldots, p_{nz}]^T$ by concatenating the position vector of all nodes.

Two nodes connected by an edge are called adjacent nodes. N_(adj(i)) is a set of nodes adjacent to node i. adjacent nodes meet at a node called an adjacent edge.

B. Inverse Kinematics

In this work, inverse kinematics is going to be used to check the feasibility of a linear actuator. In case of VGT, inverse kinematics is the calculation of length of edges from the position of nodes. There have been several works about general methods of solving forward and inverse VGT kinematics [12]–[14]. In this work, all nodes are concerned as control nodes and inverse kinematics is calculated simply:

$$L_k = \|p_i - p_j\| \tag{1}$$

where $\|\ \|$ denotes 2-norm and L_k denotes the joint parameter, length of edge $e_k = \{i, j\}$. By taking the derivative of Eq. (1), the linear relation between the velocity of the edge length, L, and node velocity x $\dot{x}$ can be obtained as follows:

$$\dot{L}_k = \frac{(p_i - p_j)^T \dot{p}_i + (p_j - p_i)^T \dot{p}_j}{L_k} \tag{2}$$

By calculating the above equation for every edge, we can relate the velocity of all edges and nodes via the matrix form, as follows:

$$\dot{L} = R\dot{x} \tag{3}$$

where each row of R is calculated from Eq. (2).

III. Locomotion Algorithm

A. Description of Rolling Locomotion

Our locomotion objective is for the VGT's center of mass to follow the desired trajectory via rolling motion without ground impact. We assume that the VGT moves slowly enough to be quasi-static and has no dynamic effects. Thus, the static stability criteria were considered and the VGT assumed to be stable when the center of mass is inside support polygon.

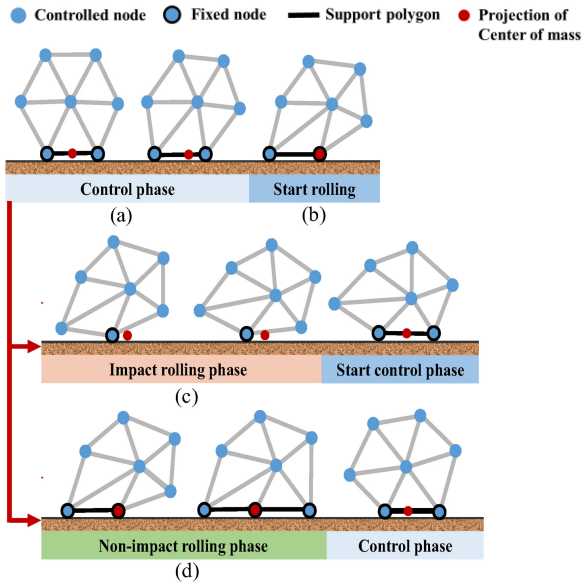

Fig. 2. Phase of rolling locomotion: (a) control phase; (b) configuration when rolling start; (c) rolling phase of impact rolling locomotion; and (d) rolling phase of non-impact rolling locomotion.

The crucial issue regarding VGT locomotion is damage prevention. A VGT is a highly sophisticated mechanical system composed of many linear actuators and specially designed spherical joints, making it weak at impact and easily damaged. Therefore, it is desirable to prevent the VGT from receiving ground impacts during rolling locomotion.

We categorize rolling motion as impact and non-impact rolling, according to whether it receives an impact from the ground. Impact and non-impact rolling motion is described in Fig. 2. Circles with black outlines are fixed nodes and length of members connecting those nodes are fixed. Since there is no external force and inertia force (assuming quasi-static), fixed nodes does not slide. Fixed nodes form a support polygon, represented as a black line. The figure is drawn in a 2D shape for simplicity; however, the actual VGT has a 3D polyhedron shape, and its support polygon literally has a polygon shape.

There are two kinds of rolling locomotion phases: control and rolling. A VGT is in the control phase when its center of mass is inside the support polygon, and it maintains its static stability as shown in Fig. 2(a). In the control phase, the position of the center of mass can be freely controlled inside the support polygon. The rolling phase begins when the center of mass is on an edge of the support polygon, as shown in Fig. 2(b), where the VGT is about to become unstable. Impact rolling and non-impact rolling moves differently during the rolling phase. In case of impact rolling, the VGT moves like a normal rolling object, as shown in Fig. 2(c). It rotates about the edge of the support polygon and tumbles to the ground via gravity. Due to fast gravitational motion, the center of mass cannot be controlled during this phase. In the case of non-impact rolling, the VGT's nodes are actively controlled so that VGT does not tumble to the ground. As in Fig. 2(d), nodes in front of the edge of the support polygon

are controlled to move forward while fixing the position of the center of mass. During both impact and non-impact rolling, the rolling phase ends when one of the controlled nodes contacts the ground and generates a new support polygon. Then, the control phase begins anew. Note that during non-impact rolling, the center of mass never goes outside the support polygon; it maintains its stability all the time. Thus, it does not impact the ground. The algorithm is described in detail in the next section.

B. Constraints

Owing to the VGT's mechanical structure, there are constraints to be considered in locomotion planning.

1) Ground Contact: The ground is modeled as a plane perpendicular to the z axis, passing through the origin. Then, the following constraint equation is given so that nodes do not overlap the ground.

$$p_{iz} \geq 0 \tag{4}$$

2) Minimum and Maximum Edge Length: Linear actuators have finite range of length; length constraint of members is set as follows.

$$L_{\min} \leq L_k \leq L_{\max} \tag{5}$$

3) Minimum Angle Between Adjacent Edges: The angle between adjacent edges cannot be smaller than a certain angle because of the mechanical limitation of the joint. The angle between adjacent edges at node i is calculated using a direction cosine. The minimum angle constraint can be written as follows.

$$\theta_{i,j,k} = \cos^{-1}\left(\frac{(p_i - p_j)^T (p_i - p_k)}{\|p_i - p_j\| \|p_i - p_k\|}\right) \geq \theta_{\min} \tag{6}$$

where j and k are adjacent nodes of node i.

4) Collision Between Non-Adjacent Edges: An edge is modeled as a cylinder with hemispheres at the ends. The diameter of the cylinder and hemisphere is equally set to d. Then, the collision detection problem becomes a minimum distance calculation between members. We use the analytical method presented in [15] for distance calculation. For collision avoidance, the minimum distance between any two non-adjacent edges must be larger than cylinder diameter d as follows.

$$d_{\min}(e_k, e_l) \geq \mathrm{d} \tag{7}$$

where $d_{\min}(e_k, e_l)$ denotes the minimum distance between non-adjacent members, e_k and e_l.

5) Velocity of Member: Because linear actuators in members have finite speeds, the velocity of the member is constrained and can be expressed using an inverse kinematics equation (3), as follows.

$$\dot{L} = R\dot{x} \leq \dot{L}_{\max} \tag{8}$$

C. Algorithm

In most previous studies, locomotion of the VGT was performed by giving pre-planned trajectories of nodes position for a gait cycle on a given topology [8]–[10]. Thus, the platform could only move in a certain pattern. However, this strategy cannot be applied to arbitrary trajectories or irregular terrain.

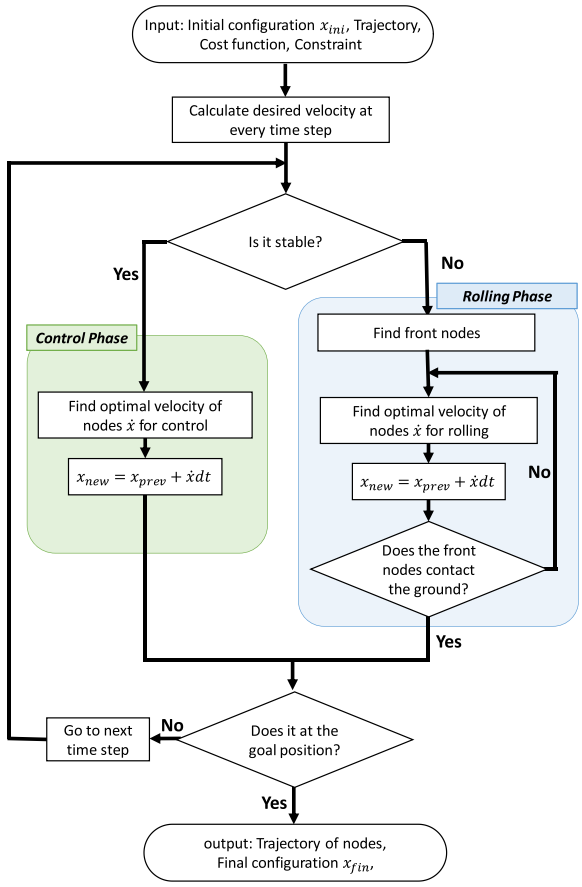

Fig. 3. Non-impact rolling locomotion algorithm.

F or more general flexible control over locomotion, Usevitch proposed an optimization-based algorithm [5]. When the configuration and desired velocity of the platform is given, this algorithm finds the optimal velocity of each node. Similarly, the velocity profile or node trajectory can be obtained by repeatedly applying the algorithm at every time step of the velocity profile of the center of mass. Using this optimization approach, this algorithm can apply to arbitrary trajectories and irregular terrain, if the information is sufficient.

Our proposed algorithm uses this optimization-based approach to implement our non-impact rolling locomotion procedure of the non-impact rolling algorithm, as represented as Fig. 3. The detailed procedure of the algorithms is as follows.

Step 1: Initialization

The initial configuration, x_{ini}, the desired trajectory of the center of mass, $x_{cm}(t)$, the cost function, J, constraints, and fixed nodes are given as input. Fixed nodes are assumed to be instantaneously fixed to the ground to form the support polygon. Then, the desired velocity, $\dot{x}_{cm}(\mathrm{t})$, is calculated by differentiating the desired trajectory, $x_{cm}(t)$.

Step 2: Stability check

Given the platform configuration, its stability is determined. If the center of mass is inside the support polygon, it is statically stable and goes into the control phase. If it is on an edge of the support polygon, it is determined to be unstable and goes to the rolling phase.

Algorithm 1: Control Phase.

1: **function** ControlPhase $(x,\ \dot{x}_{cm})$
2: $D = []$
3: $Feasible = False$
4: **while** $Feasible = False$ **do**
5: $\dot{x}_{temp} = Control\ Motion(D, x,\ \dot{x}_{cm})$
6: $x_{new} = x + \dot{x}_{temp} dt$
7: $Active = 0$
8: **for** $i = 1$ to $N_{constraints}$ **do**
9: **if** $Constraints_i(x_{new})$ **do**
10: $\mathrm{D} = [\mathrm{D}; \frac{\partial f_i(x)}{\partial x}]$
11: $Active = Active + 1$
12: **end if**
13: **end for**
14: **if** $Active == 0$ **then**
15: $Feasible = False$
16: **end if**
17: **end while**
18: $x(t + dt) = x_{new}$
19: **end function**

Step 3-1: Control phase

In the control phase, the velocity of nodes is optimized to move the center of mass at a desired velocity. The optimization algorithms in [5] are applied at this phase, as represented in Algorithm 1. The optimization problem, "ControlMotion," on line 5 of Algorithm 1 is iteratively solved until all constraints are satisfied.

$$\begin{aligned} \min_{\dot{x}} \quad & \|J(\dot{x})\|^2 \\ \text{Subject to} \quad & \mathrm{C}\dot{x} = 0, \quad \mathrm{M}\dot{x} = \dot{x}_{cm}, \\ & \mathrm{R}\dot{x} \le \dot{L}_{\max}, \quad \mathrm{D}\dot{x} \le 0 \end{aligned} \tag{9}$$

The optimization variable is a node velocity vector, $\dot{x}$.

$\mathrm{C}\dot{x} = 0$ constrains the motion of the fixed node. C is the matrix representing the contact model with the environment. Thus, the number of rows in matrix C is same as the total number of coordinates of the fixed nodes. Each row of C has only one non-zero entities, corresponding to the coordinate of a fixed node.

$\mathrm{M}\dot{x} = \dot{x}_{cm}$ causes the center of mass to follow the desired velocity, $\dot{x}_{cm}$. If we assume the mass is concentrated on the nodes, the center of mass can be represented with matrix $\mathrm{M}\dot{x}$, where $\mathrm{M} \in \mathbb{R}^{3\times 3n}$ is the matrix that transforms the node positions to the position of the center of mass.

$\mathrm{R}\dot{x} \le \dot{L}_{\max}$ constrains the speed of member length.

$$J(\dot{x}) = \left\|\dot{L}\right\| = \|R\dot{x}\| \tag{10}$$

Step 3-2: Rolling phase

The configuration during the non-impact rolling phase and its related terms are described in Fig. 4. In the figure, "rolling edge" denotes the edge of the support polygon, upon which the center of mass exists. Front node N_{front} denotes the controlled nodes located at the outer surface of the VGT and in front of the

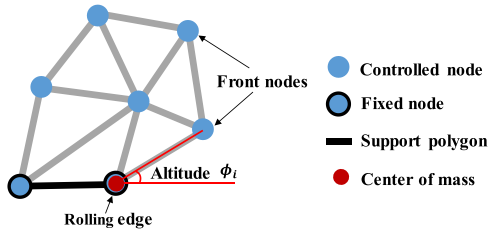

Fig. 4. Configuration at rolling phase.

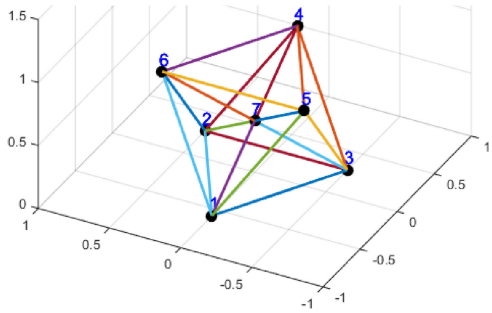

Fig. 5. Initial configuration of octahedron.

Algorithm 2: Rolling Phase.

1: **function** Rolling Phase$(x, N_{rolling})$
2: $Rolling = True$
3: $N_{front} = \text{Find Front Node}(x, N_{rolling})$
4: **while** $Rolling = True$ **do**
5: $D = []$
6: $Feasible = False$
7: **while** $Feasible = False$ **do**
8: $\dot{x}_{temp} = Rolling\ Motion(D, x, N_{front})$
9: $x_{new} = x + \dot{x}_{temp} dt$
10: $Active = 0$
11: **for** $i = 1$ to $N_{constraints}$ **do**
12: **if** $Constraints_i(x_{new})$ **do**
13: $\mathrm{D} = [\mathrm{D}; \frac{\partial f_i(x)}{\partial x}]$
14: $Active = Active + 1$
15: **end if**
16: **end for**
17: **if** $Active == 0$ **then**
18: $Feasible = False$
19: **end if**
20: **end while**
21: $x(t + dt) = x_{new}$
22: $t = t + dt$
23: **for** i $= N_{front}$ **do**
24: **if** Contact Ground(x_{new}, i) **then**
25: $Rolling = False$
26: $N_{fixed} = [N_{rolling}\ i]$
27: **break**
28: **end if**
29: **end for**
30: **end while**
31: **end function**

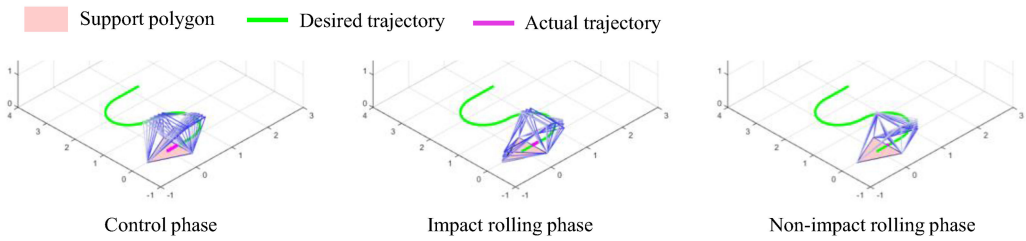

Fig. 6. Phase of non-impact rolling locomotion.

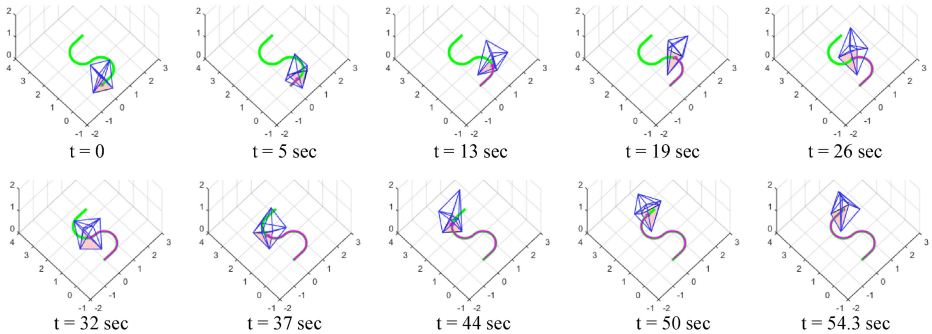

Fig. 7. Trajectory following by non-impact rolling locomotion.

rolling edge. Altitude ϕ_i is defined as the angle between node i (i.e., the perpendicular foot of node i to the rolling edge) and the projection of node i to the ground.

During the rolling phase, the center of mass is fixed, and the configuration of the platform transforms so that one of the controlled nodes contacts the ground in front of the rolling edge. The algorithm of the rolling phase is represented by Algorithm 2. The optimization problem, "RollingMotion," on line 8 of Algorithm 2, has the same control phase form as (9), except that $\dot{x}_{cm}$ is set to 0 to fix the center of mass. The cost function of the rolling phase makes the front nodes move toward the ground in front of the rolling edge, represented as follows.

$$J(\dot{x}) = \min(\{\phi_i | i \in N_{front}\} \tag{11}$$

As in the control phase, when the optimal velocity of nodes is found, the node's position at the next time step is calculated numerically. If a front node contacts the ground, the rolling phase finishes, and we go to step 2. Otherwise, we go to the next time step and optimize the velocity of nodes to minimize minimum altitude.

IV. Simulation

A simulation of impact-rolling and non-impact rolling locomotion is conducted to verify the proposed algorithm. During the rolling phase of impact rolling, the VGT tumbles to the ground dynamically. Here, we assume that the lengths of the edges are fixed during the rolling phase. This dynamic motion is obtained by solving the dynamic equation, in which the system is modeled as an inverted pendulum [8], [16].

A regular octahedron topology with 7 nodes and 18 edges was used for simulation. Its initial configuration is presented in Fig. 5. Constraint are set as; min. edge length 0.5 m, max. edge length 1.5 m, min. angle 10°, min. distance 0.1 m, max. edge velocity 0.2 m/s. Desired trajectory was set as S-shaped one formed by a straight line and a curve. The speed of center of mass was set as 0.1 m/s and time step was set as 0.1 s

Fig. 6 shows the motion of the control and the rolling phases. In the figure, the lighter VGT's color represent the VGT at the prior time. During the control phase, the VGT follows the desired trajectory within the support polygon until the center of mass touches an edge of the support polygon. During the rolling phase of impact rolling, the VGT loses stability and tumbles to the ground. Note that the center of mass goes outside of the support polygon. During the rolling phase of non-impact rolling, the front nodes move forward to contact the ground while the center of mass is fixed.

Fig. 7 shows the motion trajectory of non-impact rolling, and Fig. 8 shows minimum and maximum edge lengths, minimum angle between adjacent edges, and minimum distance between non-adjacent edges during non-impact rolling locomotion. As shown in the figures, the octahedron-shaped VGT successfully follows the desired trajectory, satisfying the constraints

Fig. 9 shows the stability margin of impact and non-impact rolling locomotion. The stability margin is defined as the minimum distance between the center of mass and the edges of the support polygon. In Fig. 9, the negative sign is assigned to the stability margin when the center of mass is outside of the support polygon. Generally, a larger stability margin corresponds to a more stable platform. In the case of impact rolling, the stability margin drops below zero during the rolling phase, causing instability and tumbling. In the case of non-impact rolling, the stability margin never drops below zero and maintains stability. Thus, non-impact rolling never loses control and prevents tumbling and ground impact.

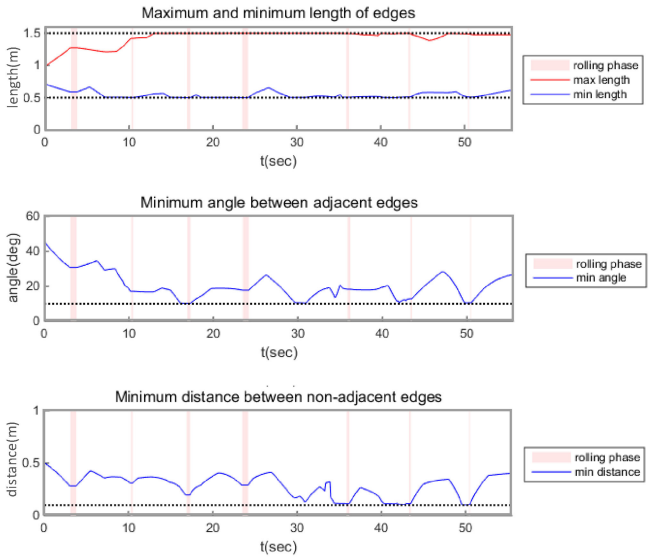

Fig. 8. Constraint related values in non-impact rolling locomotion. Dotted line indicate boundary of constrain.

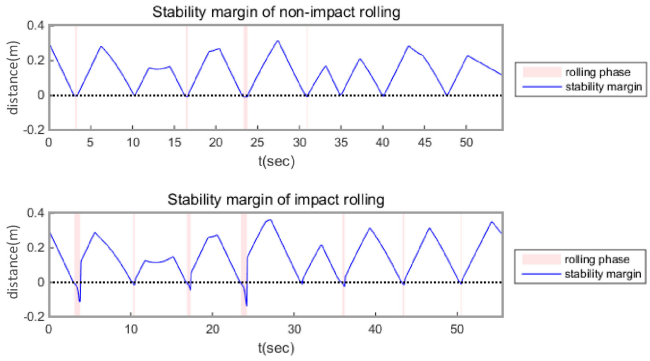

Fig. 9. Stability margin.

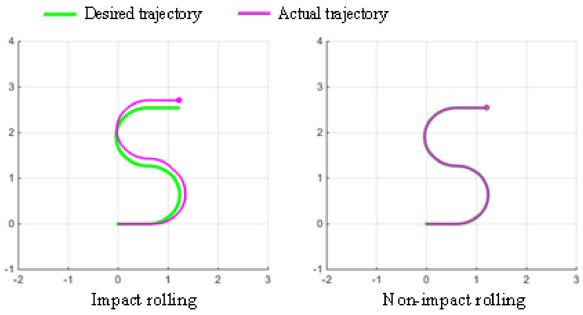

Fig. 10. Trajectory following of impact rolling and non-impact rolling.

Fig. 10 shows the top view of the desired trajectory and the actual trajectory. Impact rolling has an apparent position error with the desired trajectory. This error is generated during the rolling phase when the VGT loses control. However, non-impact rolling accurately follows the desired trajectory by maintaining stability. Therefore, non-impact rolling not only prevents the VGT from impacting the ground, it also causes it to accurately follow the desired trajectory.

V. Conclusion

This study proposed an optimization-based non-impact rolling locomotion algorithm for damage prevention. Two kinds of phases occur during rolling locomotion: control and rolling phase. A simulation of non-impact rolling locomotion was conducted with an octahedron-shaped VGT and compared with impact rolling locomotion. Our simulation showed that non-impact rolling prevented ground impacts and allowed the VGT to accurately follow the desired trajectory.

In this study, it was assumed that the VGT moves on flat surface quasi-statically. In the future, we are going to consider dynamic effect to be applicable to fast motion. Locomotion on the various terrain will also be studied based on previous works about locomotion on uneven terrain, slope and obstacles. [4], [17], [18].

References

[1] G. O. Young, "Variable geometry truss and its application to deployable truss and space crane arm," *Acta Astronaut.*, vol. 12, no. 7/8, pp. 599–607, 1985.
[2] P. C. Hughes, W. G. Sincarsin, and K. A. Carroll, "Trussarm—A variable geometry truss manipulator," *J. Intell. Mater. Syst. Struct.*, vol. 2, no. 2, pp. 148–160, 1991.
[3] G. J. Hamlin and A. C. Sanderson, "Tetrobot: A modular approach to parallel robotics," *IEEE Robot. Autom. Mag.*, vol. 4, no. 1, pp. 42–50, Mar. 1997.
[4] S. Curtis *et al.*, "Tetrahedral robotics for space exploration," in *Proc. IEEE Aerosp. Conf.*, 2007, pp. 1–9.
[5] A. Lyder, R. F. M. Garcia, and K. Støy, "Mechanical design of odin an extendable heterogeneous deformable modular robot," in *Proc. IEEE/RSJ Int. Intell. Robots Syst.*, 2008, pp. 883–888.
[6] A. Y. N. Sofla, D. M. Elzey, and H. N. G. Wadley, "Shape morphing hinged truss structures," *Smart Mater. Struct.*, vol. 18, no. 6, 2009, Art. no. 065012.
[7] A. Spinos, D. Carroll, T. Kientz, and M. Yim, "Variable topology truss: Design and analysis," in *Proc. IEEE/RSJ Int. Conf. Intell. Robots Syst.*, 2017, pp. 2717–2722.
[8] W. H. Lee and A. C. Sanderson, "Dynamic rolling locomotion and control of modular robots," *IEEE Trans. Robot. Autom.*, vol. 18, no. 1, pp. 32–41, Feb. 2002.
[9] M. Abrahantes, A. Silver, and L. Wendt, "Gait design and modeling of a 12-tetrahedron walker robot," in *Proc. 39th Southeastern Symp. Syst. Theory*, 2007, pp. 21–25.
[10] M. Abrahantes, L. Nelson, and P. Doorn, "Modeling and gait design of a 6-tetrahedron walker robot," in *Proc. 42nd Southeastern Symp. Syst. Theory*, 2010, pp. 248–252.
[11] N. Usevitch, Z. Hammond, S. Follmer, and M. Schwager, "Linear actuator robots: Differential kinematics, controllability, and algorithms for locomotion and shape morphing," in *Proc. IEEE/RSJ Int. Conf. Intell. Robots Syst.*, 2017, pp. 5361–5367.
[12] S. Jain and S. N. Kramer, "Forward and inverse kinematic solution of the variable geometry truss robot based on an n-celled tetrahedron-tetrahedron truss," *J. Mech. Des.*, vol. 112, no. 1, pp. 16–22, 1990.
[13] F. Naccarato and P. Hughes, "Inverse kinematics of variable-geometry truss manipulators," *J. Field Rob.*, vol. 8, no. 2, pp. 249–266, 1991.
[14] P. H. Tidwell, C. F. Reinholtz, H. H. Robertshaw, and C. G. Horner, "Kinematic analysis of generalized adaptive trusses," in *Proc. Joint US/Jpn. Conf. Adaptive Struct.*, 1991, pp. 772–791.
[15] V. J. Lumelsky, "On fast computation of distance between line segments," *Inf. Process. Lett.*, vol. 21, no. 2, pp. 55–61, 1985.
[16] P. Gorce and N. Rezzoug, "Numerical method applied to object tumbling with multi-body systems," *Comput. Mech.*, vol. 24, no. 6, pp. 426–434, 2000.
[17] L. H. Chen *et al.*, "Inclined surface locomotion strategies for spherical tensegrity robots," in *Proc. IEEE/RSJ International Int. Conf. Intell. Robots Syst.*, 2017, pp. 4976–4981.
[18] Y. Li, Y. A. Yao, and Y. He, "Design and analysis of a multi-mode mobile robot based on a parallel mechanism with branch variation," *Mech. Mach. Theory*, vol. 130, pp. 276–300, 2018.